

See discussions, stats, and author profiles for this publication at: <https://www.researchgate.net/publication/234006214>

Behavior of FRP Retrofitted Joints Built with Plain Bars and Low-Strength Concrete

Article in *Journal of Composites for Construction* · June 2011

Impact Factor: 2.48 · DOI: 10.1061/(ASCE)CC.1943-5614.0000156

CITATIONS

19

READS

92

3 authors:



[Alper Ilki](#)

Istanbul Technical University

151 PUBLICATIONS **575** CITATIONS

[SEE PROFILE](#)



[Idris Bedirhanoglu](#)

Dicle University

38 PUBLICATIONS **106** CITATIONS

[SEE PROFILE](#)



[Nahit Kumbasar](#)

Istanbul Technical University

64 PUBLICATIONS **439** CITATIONS

[SEE PROFILE](#)

Behavior of Deficient Joints with Plain Bars and Low-Strength Concrete

by Idris Bedirhanoglu, Alper Ilki, Santiago Pujol, and Nahit Kumbasar

Two series of tests of exterior beam-column joints were conducted. In the first series of tests, the longitudinal reinforcement of the beam was anchored in the joint with 90-degree hooks. In the second series, hooks of top bars were welded to hooks of bottom bars. Parameters varied from one test to the next and included axial load, amount of joint reinforcement, and displacement history. All of the test specimens were fabricated using low-strength concrete and plain bars to represent the conditions of joints of existing deficient reinforced concrete building structures. The test results indicate that the strengths of the specimens in Series 1 were limited by the slip of beam reinforcement at its anchorage. While the lateral load resistance of the specimens in Series 2 was higher, the nominal capacities of the column and the beam were not reached because of the combined effects of shear and slip of bars in the joint. Despite the observed damage, all of the specimens sustained their capacity to carry lateral loads during static displacement reversals with maximum drift ratios up to 4%.

Keywords: beam-column connections; low-strength concrete; plain round bar; reinforced concrete; shear; slip.

INTRODUCTION

During earthquakes, buildings have suffered damage that has been attributed to the use of low-strength concrete, plain reinforcing bars, and insufficient transverse reinforcement in beam-column joints.¹ In developing countries, structures with these features are common,¹ but research on the subject is limited.

The literature about beam-column joints built with normal-strength concrete and deformed bars is rich.²⁻²² Some of the first tests on beam-column joints were conducted by Hanson and Conner² and Hanson.³ Several equations for the design of joints were proposed based on their work. Anchorage of reinforcement in a joint was studied by Marques and Jirsa,⁴ Soroushian et al.,⁵ and Meinheit and Jirsa⁶ investigated the effect of various parameters on the shear strength of joints, including the amount of transverse and longitudinal reinforcement, column axial load, geometrical proportions, and presence of transverse beams. They concluded that transverse and longitudinal reinforcement and transverse beams increased the shear strength of the joint. Column axial load and the geometrical proportions of connections were not observed to affect the shear strength of the joint. Townsend and Hanson²⁰ also investigated the effect of column axial load and they observed that, in case of column axial tension, hysteresis loops were thinner compared to the case of column axial compression. Tsonos²¹ studied the influence of axial load variations and the $P-\Delta$ effect on the behavior of exterior beam-column joints and suggested that the $P-\Delta$ effect during a seismic-type loading increases shear stresses in the joint. Uzumeri²² reported that loading history does not affect the strength but it affects the stiffness of joints. Ehsani

and Wight⁷ also observed the positive effect of transverse beams and slabs on the shear strength of beam-column joints. They concluded that the effect of joint reinforcement is more significant in the case of joints without transverse beams and slabs. Tsonos et al.⁸ tested 20 beam-column joints under lateral-load reversals to investigate the effect of inclined joint reinforcement and observed that such reinforcement was efficient in increasing the resistance of the joints. Higazy et al.⁹ tested joints of beams and columns with compressive and tensile axial loads. It was observed that the joints of the columns in tension were not as tough as those of columns in compression. Gencoglu¹⁰ reported that the use of hoops, together with steel fibers, increased the toughness of the joints.

Compared to the case of joints built with deformed bars, there are fewer studies on the behavior of joints built with plain round bars.^{23,24} Pampanin et al.²³ tested six beam-column connections, two of which were exterior joints. The test specimens were constructed with normal-strength concrete (24 MPa [3500 psi]) and plain round bars anchored in the joint with 135-degree hooks. Studies on the bond-slip behavior of plain bars included those described in References 25 to 33. Among all of the studies reviewed, none included cases of joints built with plain reinforcing bars and low-strength concrete ($f_c' < 10$ MPa [≈ 1500 psi], f_c' is the standard cylinder compression strength of concrete). The experiments described herein were designed to investigate the behavior of exterior beam-column joints constructed with low-strength concrete and plain round bars and its sensitivity to column axial load, displacement history, amount of joint reinforcement, the presence of a transverse beam and a transverse slab, and the conditions of anchorage within the joint. The specimens represent corner joints of existing deficient reinforced concrete buildings.

RESEARCH SIGNIFICANCE

Reinforced concrete buildings built with low-strength concrete ($f_c' < 10$ MPa [≈ 1500 psi]) and plain reinforcing bars are common in Turkey.¹ Many large cities in Turkey, such as Istanbul, are located in active seismic regions. These two facts lead to the obvious question of whether joints built with low-strength concrete and plain bars should be of concern. The authors address this question by examining results from static tests. Projection of the results obtained herein to applications related to seismic loads requires careful consideration of the effects of dynamic loads.

ACI Structural Journal, V. 107, No. 3, May-June 2010.

MS No. S-2008-350.R3 received June 11, 2009, and reviewed under Institute publication policies. Copyright © 2010, American Concrete Institute. All rights reserved, including the making of copies unless permission is obtained from the copyright proprietors. Pertinent discussion including author's closure, if any, will be published in the March-April 2011 *ACI Structural Journal* if the discussion is received by November 1, 2010.

ACI member **Idris Bedirhanoglu** is a PhD Student and Research Assistant at Istanbul Technical University, Civil Engineering Faculty, Structural and Earthquake Engineering Laboratory, Istanbul, Turkey. He is also a Visiting Scholar at Purdue University, West Lafayette, IN. He received his BS from Dicle University, Diyarbakir, Turkey, and his MS from Harran University, Sanliurfa, Turkey. His research interests include behavior, retrofitting, and testing of structures under earthquake loads.

Alper Ilki is an Associate Professor at Istanbul Technical University. He is also Co-Director of the Structural and Earthquake Engineering Laboratory of Istanbul Technical University. His research interests include behavior and retrofitting of reinforced concrete members under earthquake loads.

ACI member **Santiago Pujol** is an Assistant Professor of structural engineering at Purdue University. He is a member of ACI Committee 314, Simplified Design of Concrete Buildings, and Joint ACI-ASCE Committees 441, Reinforced Concrete Columns, and 445, Shear and Torsion.

Nahit Kumbasar is an Emeritus Professor of Istanbul Technical University. His research interests include design of reinforced concrete structures and finite-element analysis of reinforced concrete members.

DESIGN OF TEST SPECIMENS

Nine specimens were tested as part of the study described in Reference 34. Details of the specimens are given in Table 1. The specimens were designed to represent the joint of a column and the two beams at a corner of an intermediate floor in a reinforced concrete building. The specimens consisted of a column and a beam perpendicular to it. One-half of the column represented the lower half of a hypothetical upper-story column. The other half of the column represented the upper half of a hypothetical lower-story column. The

specimens were supported at the ends of the column and static lateral load reversals were applied to the beam. These loads were parallel to the plane formed by beam and the column. Eight out of the nine specimens tested included a segment of a slab and a beam stub perpendicular to both the main beam and the column (Fig. 1). The intersection between the column and the beam is referred to as the beam-column joint. Properties of materials and details were chosen to represent those of structures built in Turkey before 1990.¹

Columns and beams were designed following recommendations given in the Turkish Seismic Design Code³⁵ and Building Code Regulation TS500³⁶ to avoid their failure under shear forces. Specimen JO3 was proportioned following recommendations given in the Turkish Seismic Design Code³⁵ for the design of the joint. Those provisions were not followed in the design of other specimens. Requirements from the Turkish Seismic Design Code³⁵ and TS500³⁶ followed in the design of the specimens include:

1. Beams and columns should be designed to reach their flexural capacities before their shear capacities
2. The ratio of column-to-beam flexural strength M_r should satisfy Eq. (1).

$$M_r = \frac{\sum M_c}{\sum M_b} \geq \frac{6}{5} \quad (1)$$

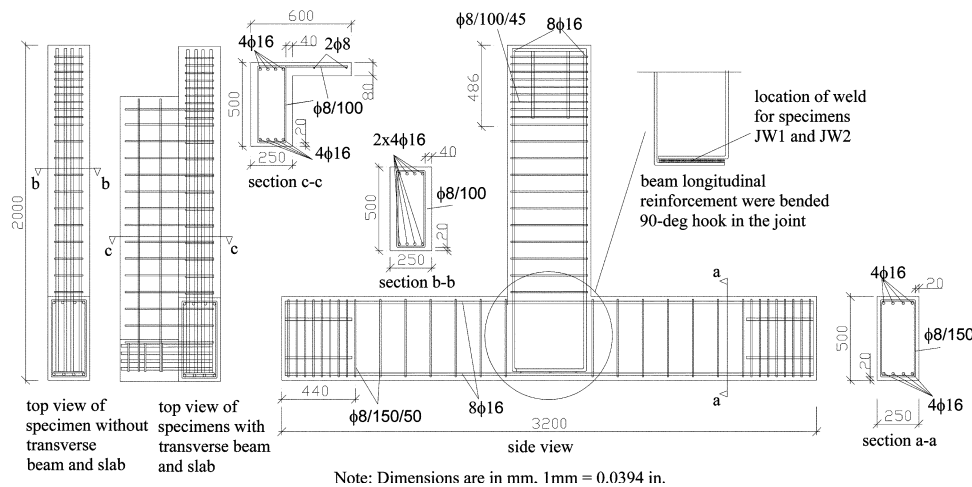


Fig. 1—Geometry and reinforcement details of specimens.

Table 1—Specimen details

Series	No.	Specimen	Age, days	f'_c , MPa	Joint reinforcement	Transverse beam and slab	Welding of hooks of beam's longitudinal bars at its anchorage in the joint	Axial load ratio, %*	Displacement history†
1	1	JO1	164	8.3	No	Present	Absent	12.5	1
	2	JO2	171	8.3	1φ8	Present	Absent	0	1
	3	JO3	179	8.3	4φ8	Present	Absent	0	1
	4	JO4	143	8.3	No	Present	Absent	50	2
	5	JO5	156	8.3	No	Absent	Absent	12.5	1
	6	JO6	176	8.3	No	Present	Absent	0	1
	7	JO7	197	8.3	No	Present	Absent	50	1
2	8	JW1	208	8.3	No	Present	Present	12.5	1
	9	JW2	230	8.3	No	Present	Present	12.5	1

*Computed using Eq. (3).

†Displacement history 2 is described in Fig. 4(a) and displacement history 1 is described in Fig. 4(b).

Note: 1 MPa = 145 psi.

In this equation, ΣM_c and ΣM_b are the sums of the nominal moment capacities of columns and beams at the faces of the joint, respectively. This ratio was larger than 1.8 for all specimens.

3. The development length l_{dh} for plain round bars with 90-degree hooks should exceed

$$l_{dh} = \frac{3}{4} \left(0.24 \frac{f_y}{f_{ct}} \phi \right) \geq 40\phi \quad (2)$$

In Eq. (2), f_y is the unit stress at yield, f_{ct} is the tensile strength of concrete, and ϕ is the diameter of the reinforcement. In all of the specimens, the longitudinal reinforcement of the column was continuous and the longitudinal reinforcement of the beam was anchored in the joint using 90-degree hooks. The anchorage length (measured along the bar including the length of the hook) was 880 mm (35 in.), which corresponds to 55 bar diameters. Assuming that f_{ct} is $0.35\sqrt{f'_c}$ MPa ($4\sqrt{f'_c}$ psi), Eq. (2) yields a required anchorage length of 950 mm (37.4 in.), which corresponds to 60 bar diameters. In the beams of Specimens JW1 and JW2, the hooks of top longitudinal bars were welded to the hooks of bottom bars. To place these welds, an 80 mm (3.2 in.) thick layer of concrete was removed after the construction of Specimen JW1. For Specimen JW2, a 130 mm (5.1 in.) thick layer of concrete was removed. After welding, the removed concrete was replaced with high-strength repair mortar. It should be noted that both the top and bottom plain round bars of the beams were generally terminated with a 90-degree hook in the joint core in Turkey between the mid-1970s and 1990s before deformed bars were common. Welding was investigated as a potential rehabilitation technique for corner joints.

TEST PROGRAM

Test specimens

Two series of specimens were tested to evaluate their behavior under static lateral displacement reversals (Table 1). The specimens were constructed with low-strength concrete (the measured cylinder strength was $f'_c = 8.3$ MPa [$f'_c = 1200$ psi]) and plain round reinforcing bars. Except for JO2 and JO3, the specimens had no hoops in the beam-column joint (Table 1). Details of the reinforcement are shown in Fig. 1. Columns and beams had 250 x 500 mm (9.8 x 19.7 in.) cross sections and were reinforced with 8 ϕ 16 bars

Table 2—Concrete mixture proportions, kg/m³

Concrete	Aggregate size, mm	Cement	Water	Sand	Crushed stone	Coarse aggregate	High-range water-reducing admixture
Normal-weight	8	170	239	698	414	747	1.8

Note: 1 kg/m³ = 0.06243 lb/ft³; 25.4 mm = 1 in.

Table 3—Mechanical properties of reinforcing bars

Reinforcement	Diameter, mm (in.)	f_y , MPa (ksi)	$\epsilon_y = f_y/E_s$	ϵ_{sh}	f_{smax} , MPa (ksi)	ϵ_{smax}	f_{su} , MPa (ksi)	ϵ_{su}
ϕ 16	16 (0.63)	333 (48)	0.0017	0.03	470 (68)	0.20	335 (49)	0.34
ϕ 8	8.4 (0.31)	315 (46)	0.0016	0.03	433 (63)	0.20	265 (38)	0.33

*Maximum measured deviations from nominal diameter: ± 0.2 mm (± 0.008 in.).

†Mechanical characteristics are determined by averaging test results obtained from five specimens.

in the longitudinal direction. The ratio of the total cross-sectional area of longitudinal reinforcement to gross cross-sectional area was 1.3% for both beams and columns. Slabs were reinforced with 2 ϕ 8 bars parallel to the beam (Fig. 1). The transverse reinforcement in the columns consisted of 8 mm (0.3 in.) closed ties at a spacing of 150 mm (5.9 in.). The transverse reinforcement in the beams was 8 mm (0.3 in.) closed ties at a spacing of 100 mm (3.9 in.). The concrete cover over transverse reinforcement was 20 mm (0.8 in.) thick. Other properties of the specimens are given in Table 1. In this table, axial load ratios v are calculated using Eq. (3), where b and h are the width and depth of the cross section of the column and P is the axial load.

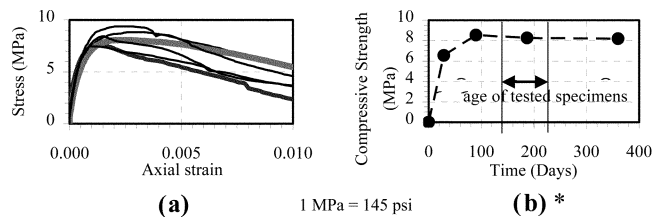
$$v = \frac{P}{bhf'_c} \quad (3)$$

Concrete

To represent typical conditions in structures built in Turkey before 1990,¹ the concrete was designed to reach a compressive strength of approximately 10 MPa (≈ 1500 psi). The concrete mixture proportions are given in Table 2. All of the specimens were cast in the Structural and Earthquake Engineering Laboratory of Istanbul Technical University on December 17, 2006. The compressive strength measured 180 days after casting was 8.3 MPa (1200 psi). The modulus of elasticity was 13,000 MPa (1900 ksi). These values are means of results from six standard cylinder tests. Stress-strain relationships measured 180 days after casting and the measured variation of strength with time are shown in Fig. 2(a) and (b), respectively. Standard cylinder strengths varied between 7.4 and 9.4 MPa (1070 and 1360 psi) at the age of 180 days. Joint specimens were tested from 140 to 230 days after casting (Fig. 2(b), Table 1).

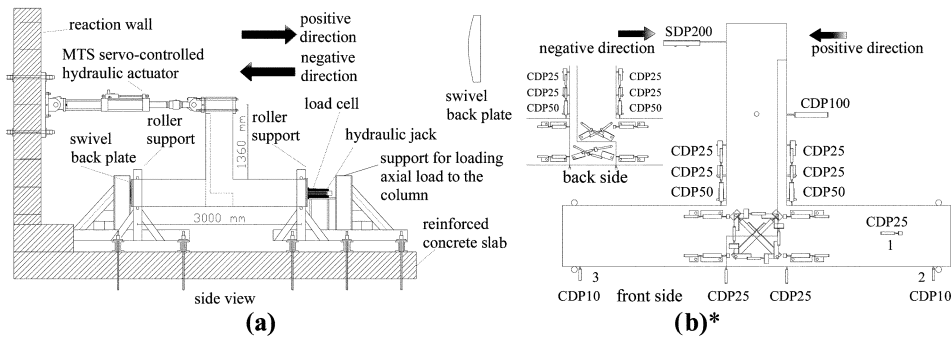
Reinforcement

Plain 16 mm (0.63 in.) diameter bars were used as longitudinal reinforcement in both beams and columns. Plain 8 mm (0.31 in.) diameter bars were used to fabricate transverse reinforcement. The mechanical properties of the longitudinal and transverse reinforcement are shown in Table 3. In this table, ϵ_y is the yield strain, E_s is the elastic modulus of steel, ϵ_{sh} is strain at the onset of strain hardening, f_{smax} is maximum stress, ϵ_{smax} is the strain corresponding to maximum stress, f_{su} is stress at rupture, and ϵ_{su} is strain at rupture measured over a gauge length of 100 mm (4 in.). All of these values are the averages of five coupon tests. Yield stresses measured for 16 and 8 mm (0.63 and 0.31 in.) diameter bars varied between 323 and 345 MPa (47 and 50 ksi) and 299 and 333 MPa (43 and 48 ksi), respectively.



*Each compressive strength value is the average of six standard cylinder tests.

Fig. 2—(a) Stress-strain relationship; and (b) strength-age relationship of concrete.



*Note: Diagonal deformations were measured with LVDTs attached to the joint forming a 45-deg and 27-deg angles with the column axis for front and back sides, respectively. These deformations were measured over a 480-mm (19 in.) and 320-mm (13 in.) for front and back sides, respectively.

Fig. 3—(a) Test setup; and (b) location of transducers.

Test setup and loading pattern

The specimens were tested under the combined action of constant axial load and static lateral load reversals. The test setup is shown in Fig. 3(a). The beam-column joint assemblies were tested with the column positioned horizontally and the beam standing vertically. The assemblies were supported by rollers at the ends of the column, as shown in Fig. 3(a). These rollers passed through the holes drilled in the steel plates that provided vertical reactions. These holes had a diameter that was 1 mm (0.018 in.) larger than the diameter of the rollers to allow rotation of column ends. Axial load and horizontal reactions were applied using a hydraulic jack at one end of the column. Three levels of axial load were applied to the column: 0, 0.125, and $0.50f'_c \times b \times h$. Lateral loads were applied monotonically and in the horizontal direction to the free end of the beam using a 250 kN (56 kips) servo-controlled hydraulic actuator. All tests were conducted under displacement control. The movements of the specimen in the vertical and horizontal directions were measured using three linear variable displacement transducers (LVDTs) (numbered as 1, 2, and 3 in Fig. 3(b)). Other instrumentation used included load cells and electrical resistance strain gauges bonded on steel reinforcement and concrete surfaces. Each test started with a gradual application of the axial load. Subsequently, lateral displacements were imposed until the selected target drift ratios were reached (Fig. 4). Drift ratios reported herein were the ratios of the displacements measured at the free end of the beam to the length of the beam. These ratios were corrected to subtract the rigid-body rotation associated with the deformations of the supports.

TEST RESULTS

Test results are described in terms of imposed drift ratios. Lateral loads applied to the beam were parallel to the longitudinal axis of the column. Loads making the slab work in tension (Fig. 3) are referred to as positive loads. Loads making the slab work in compression are referred to as negative loads. Plots of applied load versus measured load-point displacement (and drift ratio) are presented in Fig. 5 to 9. In these figures, marks indicate important stages in each test. Observe that all the curves exhibit “pinching” and the maximum load reached was larger in the positive direction for all of the specimens with a slab (Table 4). The strengths of Specimens JW1 and JW2, in which the hooks of reinforcing bars in the beam were welded to limit bar slip were, on average, 33% larger than the strength of Specimen JO1, respectively (Table 4). Specimens JW1, JW2, and JO1 were

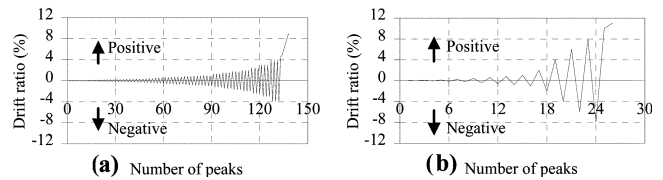


Fig. 4—Displacement history for: (a) Specimen JO4; and (b) other specimens.

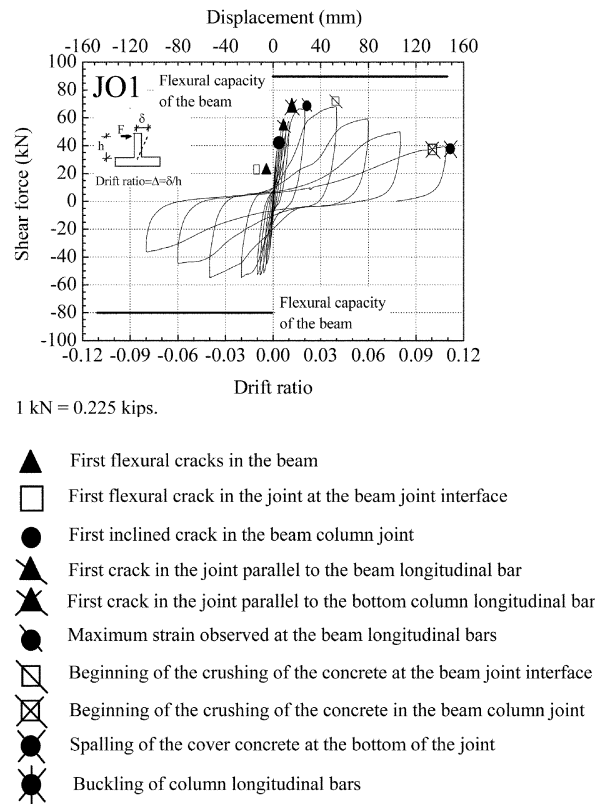


Fig. 5—Load versus deflection response for Specimen JO1.

similar except for the use of welding to improve anchorage. The strength increased with increasing amounts of joint reinforcement and increasing column axial load. But strength was less sensitive to column axial load than it was to the amount of joint reinforcement (Table 4). Specimens retained a large fraction (>90%) of their lateral load-carrying capacities during cycles at maximum drift ratios of up to 4%.

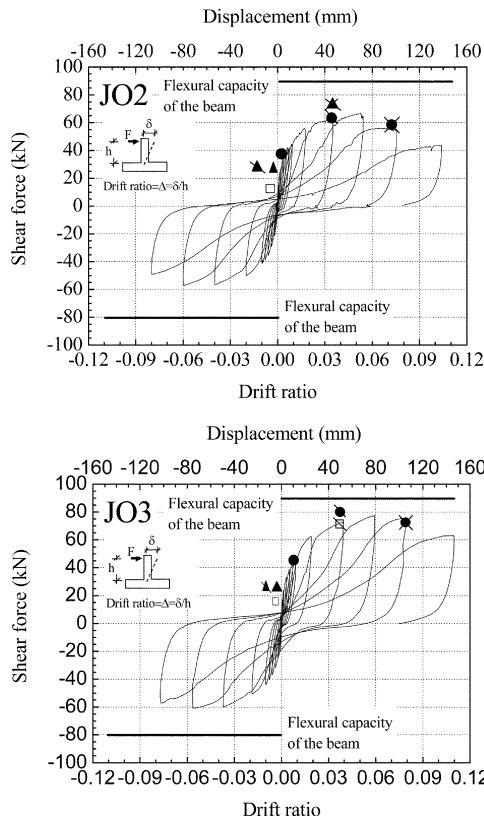


Fig. 6—Load versus deflection responses for Specimens JO2 and JO3. (Note: 1 kN = 0.2248 kip; 1 mm = 0.0394 in.)

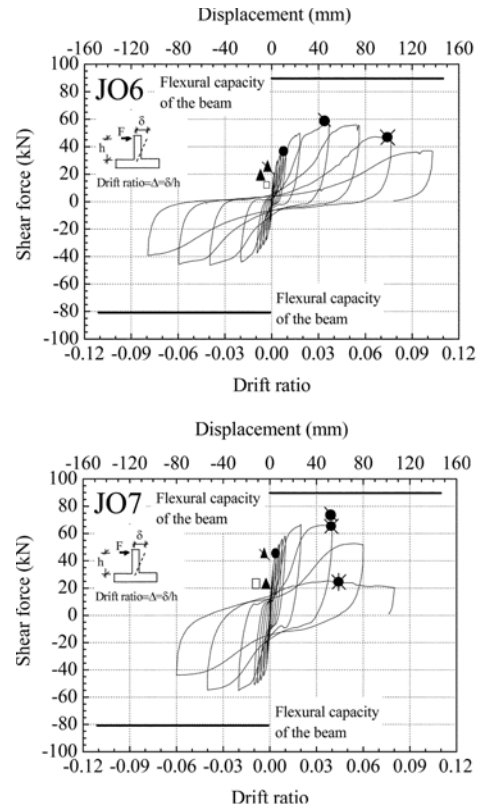


Fig. 8—Load versus deflection responses for Specimens JO6 and JO7. (Note: 1 kN = 0.2248 kip; 1 mm = 0.0394 in.)

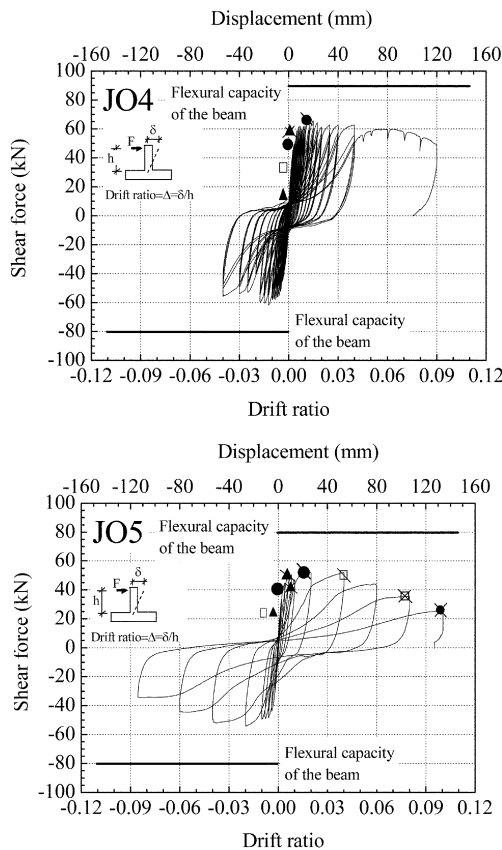


Fig. 7—Load versus deflection responses for Specimens JO4 and JO5. (Note: 1 kN = 0.2248 kip; 1 mm = 0.0394 in.)

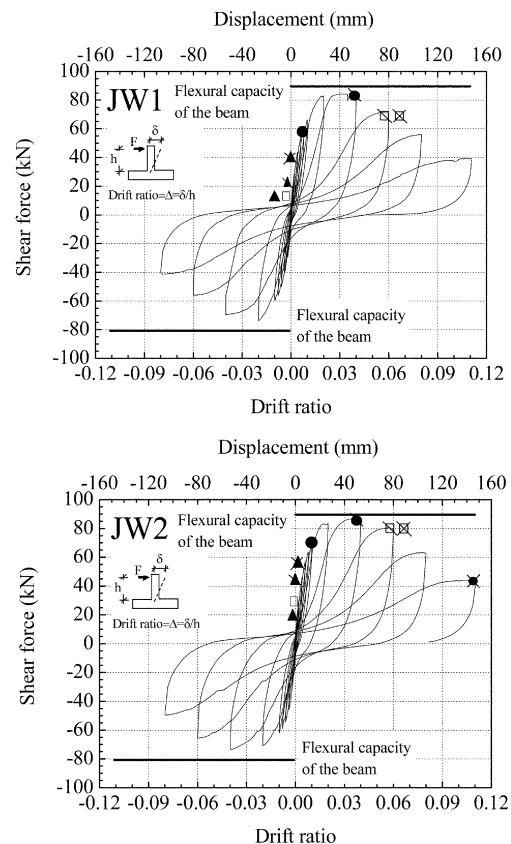


Fig. 9—Load versus deflection responses for Specimens JW1 and JW2. (Note: 1 kN = 0.2248 kip; 1 mm = 0.0394 in.)

Table 4—Test results

Specimen	Maximum load at tip of beam		Drift ratio at first		Strains in beam longitudinal reinforcement at maximum lateral load (5)	Mean unit bond stress		$\tau_b/\sqrt{f'_c}$ (slab in tension) f'_c in MPa (8)	V_{jh}/f'_c (slab in tension)
	Slab work in tension, kN (kips) (1)	Slab work in compression, kN (kips) (2)	Flexural crack (3)	Inclined crack (4)		τ_b , MPa (psi)			
					(6)	(7)			
JO1	65.8 (14.8)	53.3 (12.0)	1/1000	4/1000	0.0011	1 (145)	1.03 (149)	0.35	—
JO2	63.4 (14.2)	55.0 (12.4)	1/1000	6/1000	0.0014	1.27 (184)	0.99 (144)	0.44	—
JO3	77.5 (17.4)	61.0 (13.7)	1/1000	6/1000	0.0015	1.36 (197)	1.25 (181)	0.47	—
JO4	66.3 (14.9)	61.0 (13.7)	1/2000	7/1000	0.0010	0.91 (132)	1.04 (151)	0.32	—
JO5	51.5 (11.6)	51.4 (11.6)	1/1000	4/1000	0.0011	1 (145)	0.95 (138)	0.35	—
JO6	56.2 (12.6)	46.0 (10.3)	1/2000	6/1000	0.0011	1 (145)	0.86 (125)	0.35	—
JO7	66.6 (15.0)	55.1 (12.4)	1/1000	4/1000	0.0011	1 (145)	1.05 (152)	0.35	—
JW1	81.5 (18.3)	70.8 (15.9)	1/2000	8/1000	0.0016	—	—	—	0.23
JW2	87.0 (19.6)	73.0 (16.4)	1/1000	10/1000	0.0017	—	—	—	0.24

Notes: Column 6: Values calculated based on strain-gauge measurements. Column 7: Values computed assuming force in steel (Eq. (4)) was $F_s = M/0.9d$ where M is maximum measured moment and d is effective depth. Column 8: Values calculated based on those in Column 6; 1 MPa = 145 psi.

Table 5—Strains measured on reinforcement and diagonal deformations of joint

Specimen	Maximum tensile strains						Maximum diagonal strains in joint	
	Beam longitudinal bars	Slab longitudinal bars	Column longitudinal bars	Beam stirrups	Column ties	Joint reinforcement	Front face	Back face
JO1	0.0011	0.0019	0.00074	0.00039	0.00021	—	0.052	0.040
JO2	0.0015	0.0016	0.00096	0.00037	0.00015	0.0010	0.054	0.033
JO3	0.0015	0.0014	0.0010	0.00059	0.00016	0.00093	0.050	0.038
JO4	0.0013	—	0.00015	0.00090	0.00045	—	0.027	0.027
JO5	0.0011	—	0.00076	0.00023	0.00029	—	0.057	0.053
JO6	0.0012	—	0.0015	0.00017	0.00020	—	0.053	0.027
JO7	0.0013	—	0.00051	0.00026	0.00043	—	0.052	0.038
JW1	0.0017	—	0.00090	0.00060	0.00024	—	0.053	0.043
JW2	0.0018	—	0.0010	0.00070	0.00023	—	0.052	0.043
Mean	—	0.0016	0.00080	0.00042	0.00033	0.00097	0.050	0.038

Note: — indicates that no measurement was made.

Table 6—Lateral loads associated with computed nominal flexural and shear capacities of members of beam-column joint assemblies

Lateral load (kN [kips]) associated with nominal				
Flexural capacity			Shear capacity (computed using design provisions in ACI 318-08) ³⁷	
of beam		of column for zero axial load	of beam	of column
in positive direction	in negative direction			
90 (21)	80 (18)	200 (45)	200 (45)	340 (76)

Maximum strains measured in the beam and column reinforcement are listed in Tables 4 and 5. Notice that larger strains were measured in the reinforcement of Specimens JW1 and JW2. Maximum diagonal deformations measured on the faces of the joint are given in Table 5. Diagonal deformations were measured with LVDTs attached to the surface of joint, as shown in Fig. 3.

Crack maps obtained after the completion of cycles at drift ratios of up to 4% are presented in Fig. 10. Photographs taken at the end of the experiments are also shown in Fig. 10. In all specimens, flexural cracks were first observed in beams and slabs at drift ratios ranging from 0.05 to 0.1%. In specimens with slabs, the cracks on the slab were narrower than the cracks on the opposite side of the beam. In all specimens, inclined cracks were observed in the joint. They formed at drift ratios ranging from 0.4 to 0.7% for specimens in Series 1 and 0.8 to 1% for specimens in Series 2. Up to a

drift ratio of 4% damage concentrated at the beam-joint interface and the joint. Despite the damage, the specimens did not experience large losses in load-carrying capacity at drift ratios of up to 4%. After a drift ratio of 4%, the joints of the specimens in Series 2 were more severely damaged than the joints of specimens in Series 1 because of the increase in shear allowed by improved anchorage conditions.

DISCUSSION OF EXPERIMENTAL RESULTS

Lateral load capacities associated with the computed nominal flexural and shear capacities of the members of the beam-column joint subassemblages are given in Table 6. For specimens in Series 1, the maximum applied lateral load did not exceed 78 kN (17.5 kips) in the positive direction and 61 kN (13.7 kips) in the negative direction. Therefore, it is clear that the capacities of the specimens in Series 1 were limited by the strengths of the joints.

The fact that 1) the maximum strains measured in the longitudinal reinforcement in beams and columns for the specimens in Series 1 did not exceed the nominal yield strain; and 2) the strengths of the specimens in Series 2 (in which the hooks of beam reinforcing bars were welded) were larger than the strengths of comparable specimens in Series 1, indicated that the slip of beam reinforcement limited the strength of specimens in Series 1. Reinforcement slip was not associated with bond failure, however. Specimens retained a large fraction (>90%) of their lateral load-carrying capacities during cycles at maximum drift ratios of up to 4% (Table 7). Relative reductions in lateral load-carrying capacity at drift ratios of 4 and 6% are

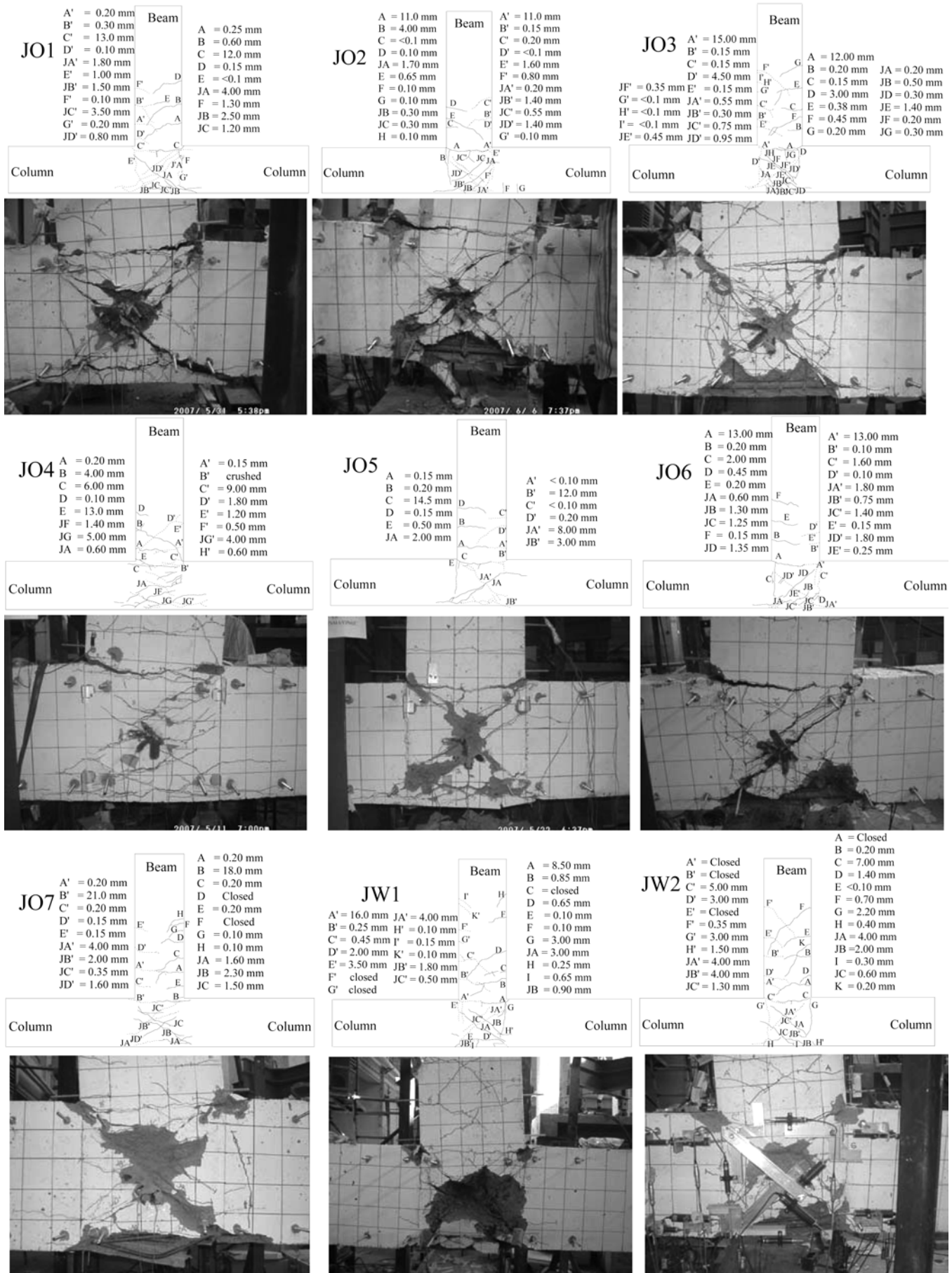


Fig. 10—Cracking patterns at 4% drift ratio and damage photos at end of tests. (Note: 1 mm = 0.0394 in.)

Table 7—Comparison of energy dissipation capacities and strength degradation

Specimens	Normalized values of energy dissipation capacities at different drift ratios										Decrease in lateral load-carrying capacity at 4 and 6% drift ratio	
	1%		3%		4%		6%		8%		4%	6%
	Per cycle	Cumulative	Per cycle	Cumulative	Per cycle	Cumulative	Per cycle	Cumulative	Per cycle	Cumulative		
JO1	0.86	0.87	0.91	0.90	0.89	0.94	0.83	0.90	0.70	0.87	0	13%
JO2	0.76	0.61	0.77	0.62	0.82	0.84	0.88	0.87	0.87	0.92	0	0
JO3	0.76	0.58	0.72	0.63	0.83	0.79	0.97	0.87	1.00	0.95	0	0
JO4	0.67	—	0.56	—	0.61	—	—	—	—	—	6%	8%
JO5	0.81	0.83	0.86	0.85	0.82	0.88	0.74	0.83	0.66	0.81	0	18%
JO6	0.61	0.52	0.68	0.61	0.65	0.68	0.71	0.72	0.67	0.74	0	1%
JO7	1.00	1.00	1.00	1.00	0.92	1.00	0.90	0.97	—	—	1%	25%
JW1	0.71	0.70	0.90	0.81	0.98	0.95	0.89	0.94	0.77	0.92	0	14%
JW2	0.73	0.68	1.00	0.85	1.00	0.98	1.00	1.00	0.87	1.00	0	8%
Value used to normalize, kNmm	658	1910	2210	4100	5220	8890	6510	15,230	6510	21,740	—	—

Note: 1 kNmm = 8.85 lbf-in.

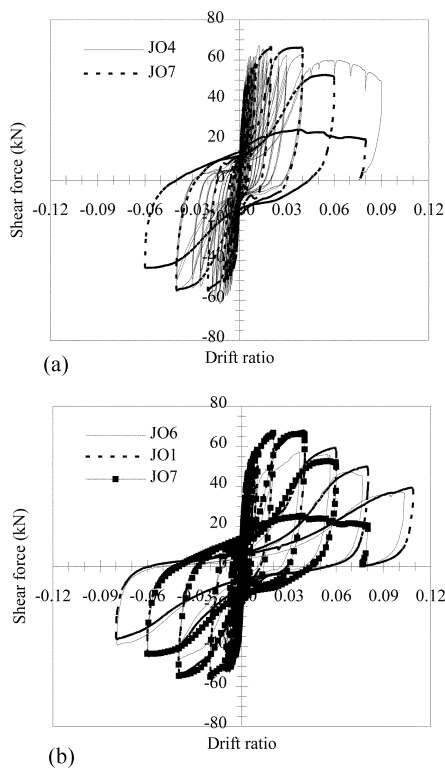


Fig. 11—Comparison of shear force-drift ratio relationships: (a) Specimens JO4 and JO7; and (b) Specimens JO6, JO1, and JO7. (Note: 1 kN = 0.2248 kip.)

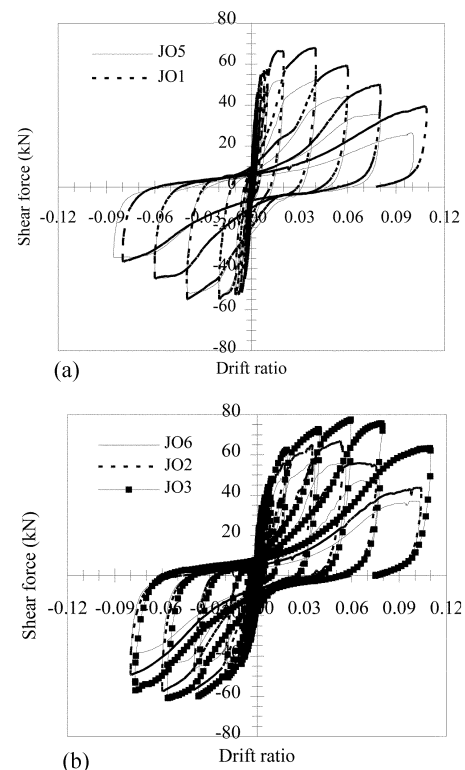


Fig. 12—Comparison of shear force-drift ratio relationships: (a) Specimens JO1 and JO5; and (b) Specimens JO6, JO2, and JO3. (Note: 1 kN = 0.2248 kip.)

given in Table 7 together with normalized values of dissipated energy. Dissipated energy was calculated as the area under the load-displacement hysteresis curves. Both cumulative energy and energy dissipated per cycle are reported. Normalization was done with respect to the maximum energy dissipated at or up to a given drift ratio among all the specimens tested. The maximum energy dissipated at or up to a given drift ratio is listed as “value used to normalize.” As seen in this table, the maximum decrease in lateral load-carrying capacity at the drift ratio of 6% was 18%.

If the bond stress is assumed to be uniformly distributed along the anchorage length of a bar embedded in concrete, the unit bond stress τ_b is given by

$$\tau_b = \frac{F_s}{\pi \phi l_{dh}} \quad (4)$$

where F_s is the force in the bar, ϕ is the diameter of the bar, and l_{dh} is the anchorage length (measured along the bar including the length of the hook). The mean of the unit bond stress maxima measured for the specimens tested was approximately $0.37 \sqrt{f'_c}$ MPa ($4.5 \sqrt{f'_c}$ psi) for Series 1 (Table 4). F_s was calculated on the basis of strains measured on the beam longitudinal bars using electrical-resistance strain gauges. The results of these computations were consistent

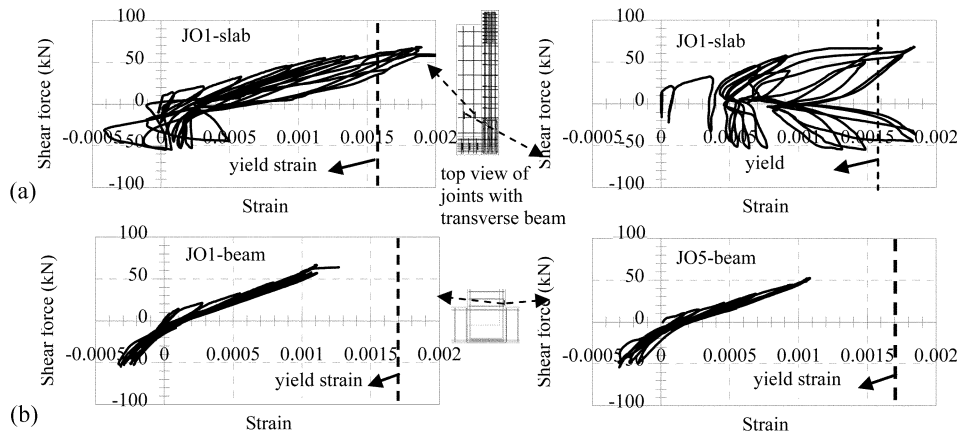


Fig. 13—Strain measured on: (a) slab reinforcement of Specimen JO1; and (b) beam longitudinal reinforcement of Specimens JO1 and JO5. (Note: 1 kN = 0.2248 kip.)

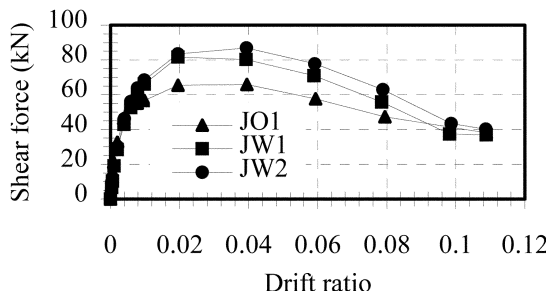


Fig. 14—Comparison of envelopes of shear force-drift ratio relationships (Specimens JO1, JW1, and JW2). (Note: 1 kN = 0.2248 kip.)

with the expected force in the reinforcement for an internal lever arm of $0.9d$ (d is effective depth).

Effect of displacement history

To test the hypothesis that the drift capacity of the test specimens could be critically affected by the displacement history chosen, two specimens that were nominally identical (J04 and J07) were tested under different displacement histories. Specimen J04 was subjected to 66 cycles at drift ratios varying gradually from 1/4000 to 1/25 (Fig. 4(a)). Specimen J07 was subjected to 10 cycles at drift ratios varying gradually from 1/4000 to 1/25 (Fig. 4(b)). Within this range, that is, for drift ratios not exceeding 1/25, both specimens sustained their capacity to carry lateral loads regardless of the number of cycles applied (Fig. 11(a)).

Effect of axial load

Specimen JO6 was tested with no additional axial load. The columns of Specimens JO1 and JO7 were subjected to axial loads corresponding to 12.5 and 50% of $f'_c \times b \times h$, respectively. The maximum lateral load for the two specimens with axial load, regardless of the level of axial load, was approximately 20% larger than the maximum lateral load reached by the specimen without axial load (Fig. 11(b)). All three specimens sustained the lateral load-carrying capacities during cycles at drift ratios of up to 4%. In the test of the specimen subjected to the highest axial load (J07), buckling of column longitudinal bars was observed in a cycle with a maximum drift ratio of 6% (Fig. 8). The energy dissipated in a cycle (the area enclosed within the load-displacement hysteresis curves and the

horizontal axis computed for different drift ratios and the cumulative dissipated energy at different drift ratios are given in Table 7. Table 7 shows that both energy dissipated in a cycle and cumulative energy increased with increases in the axial load. The hysteresis curves for Specimen J07, which had higher axial load, indeed showed less “pinching” than the curves for Specimens J01 and J06.

Effects of transverse beam stub and slab

The potential effects of transverse beams and slabs were investigated by comparing results from tests of Specimens JO1 and JO5. Specimen JO1 had a transverse beam stub and a slab; Specimen JO5 did not. The lateral load capacities of these specimens were similar (within 4% from one another) in the negative loading direction, indicating that the presence of a lateral beam and a slab did not affect the bond of the bars in the exterior joints tested (Fig. 12(a)). In the positive loading direction (in which the slab works in tension) the lateral load-carrying capacity of Specimen JO1 was approximately 30% larger than the lateral load-carrying capacity of Specimen JO5. The difference in capacity in the positive direction was related to the presence of slab reinforcement parallel to the main beam. The slab reinforcement had a smaller diameter than beam reinforcement and, therefore, better anchorage. In fact, strain gauges installed on the slab reinforcement in Specimen JO1 showed that strains in this reinforcement reached the yield strain (Fig. 13(a)). Strains in the beam longitudinal reinforcement did not exceed 0.001 (Fig. 13(b)).

Despite the fact that the joint of Specimen JO1 was subjected to larger stresses, smaller diagonal deformations (Table 5) and thinner cracks (Fig. 10) were observed on the lateral face of this joint because of the constraint caused by the transverse beam stub. As seen in Table 7, the energy dissipation capacity of Specimen JO1 was slightly higher than that of Specimen JO5.

Effect of joint reinforcement

The effect of joint reinforcement was investigated comparing results from the tests of Specimens JO6, JO2, and JO3. Specimen JO6 had no reinforcement in the joint. Specimen JO2 had one 8 mm (0.3 in.) hoop and Specimen JO3 had four 8 mm (0.3 in.) hoops in the joint. The ratio of joint reinforcement was 0.0008 for Specimen JO2 and 0.0032 for Specimen JO3. These ratios were computed as the total cross-sectional area of hoops in the joint divided by the

cross-sectional area of the joint. The hoops in the joint were parallel to the longitudinal axis of the main beam.

The use of joint reinforcement resulted in thinner inclined cracks in the joint, larger lateral load-carrying capacities (Fig. 12(b)), and larger strains in the beam longitudinal reinforcement (Table 5). But drift capacity was not observed to be critically sensitive to the amount of joint reinforcement with Specimens JO2, JO3, and JO6 reaching drift ratios in excess of 6% before they exhibited large stiffness decay. The mean of the unit bond stress maxima for longitudinal bars was computed to be $0.47\sqrt{f'_c}$ and $0.35\sqrt{f'_c}$ MPa ($5.7\sqrt{f'_c}$ and $4.2\sqrt{f'_c}$ psi) for specimens with and without joint reinforcement, respectively. As seen in Table 7, the energy dissipation capacity of Specimens JO2 and JO3 are close to each other and higher than Specimen JO6.

Effect of welding and repair mortar

The hooks of the top longitudinal bars were welded to the hooks of bottom longitudinal bars in the beams of Specimens JW1 and JW2. To place these welds, a layer of concrete surrounding the hooks was removed after construction of specimens. The removed concrete was replaced with high-strength repair mortar. As described previously, the layer of repair mortar used in Specimen JW2 was thicker than the layer used in Specimen JW1. This difference had no substantial effect on the lateral load-carrying capacities of the specimens, which differed from each other by no more than 7% (in favor of Specimen JW2). As seen in Table 7, the energy dissipation capacities of Specimens JW1 and JW2 were close to each other and higher than the capacity of a comparable specimen (Specimen JO1). But more brittle behavior was observed for welded specimens (Specimens JW1 and JW2), as shown in Fig. 14. It is likely that the more rapid decrease in load-carrying capacity was related to the effects of increased shear in the joints of the welded specimens.

CONCLUSIONS

The purpose of the investigation described herein was to evaluate the effects of column axial load, transverse beams and slabs, and joint reinforcement on the response to static load reversals of beam-column joints built with low-strength concrete (8.3 MPa [1200 psi]) and plain reinforcing bars. The ranges of the variables studied were:

- Axial load (kept constant in each test), 0.0 to 0.50;
- Transverse beam and slab, present or absent;
- Ratio of joint reinforcement (perpendicular to the column), 0 to 0.32%; and
- Anchorage conditions (welding the hooks of the top bars to hooks of the bottom bars in the beam), present or absent.

Nine beam-column assemblies were tested and the full nominal shear and flexural capacities of the framing beams and columns could not be reached.

In seven cases (Series 1), the capacity of the specimen was limited by the slip of beam reinforcement at its anchorage. Mean bond stresses were determined to have reached values ranging from approximately $0.33\sqrt{f'_c}$ to $0.50\sqrt{f'_c}$ MPa ($4\sqrt{f'_c}$ to $6\sqrt{f'_c}$ psi).

In two cases (Series 2), the anchorage of the longitudinal reinforcement of the beam was improved by welding the hooks of the top bars to the hooks of the bottom bars. The mean of the strengths of specimens with welds was 35% larger than the mean of the strengths of specimens without them. But this increase was not sufficient to allow the

column and the beam framing into the joint to reach their nominal strengths. The capacity of these specimens seems to have been limited by damage in the joint core.

The dissipated energy was larger in comparable assemblies in which columns had larger axial loads. All of the specimens sustained their capacities to carry lateral loads during static displacement reversals with maximum drift ratios of up to 4%. The maximum strength decay at 4% drift was less than 10% for all specimens (Table 7).

ACKNOWLEDGMENTS

The experimental study was funded by The Scientific and Technological Research Council of Turkey (TUBITAK), Project Number 106M054, and Istanbul Technical University, Project Number 31811. The grant provided by TUBITAK to one of the authors, I. Bedirhanoglu, to continue this research at Purdue University is gratefully acknowledged. Thanks are due to M. Sozen of Purdue University for his suggestions. The assistance of O. Incecik and K. Koclu and the valuable contribution from S. Usta, who helped in the construction of the specimens and, unfortunately, passed away recently, are gratefully acknowledged.

REFERENCES

1. Koru, B. Z., "Seismic Vulnerability Assessment of Low-Rise Reinforced Concrete Buildings," PhD thesis, Purdue University, West Lafayette, IN, 2002, 344 pp.
2. Hanson, N. W., and Connor, H. W., "Seismic Resistance of Reinforced Concrete Beam-Column Joints," *Journal of the Structural Division, ASCE*, V. 93, No. 5, 1967, pp. 533-560.
3. Hanson, N. W., "Seismic Resistance of Concrete Frames with Grade 60 Reinforcement," *Journal of the Structural Division, ASCE*, V. 97, No. 6, 1971, pp. 1685-1700.
4. Marques, J. L. G., and Jirsa, J. O., "A Study of Hooked Bar Anchorages in Beam-Column Joints," *ACI JOURNAL, Proceedings V. 72, No. 5, May 1975*, pp. 198-209.
5. Soroushian, P.; Obaseki, K.; Nagi, M.; and Rojas, M. C., "Pullout Behavior of Hooked Bars in Exterior Beam-Column Connections," *ACI Structural Journal*, V. 85, No. 3, May-June 1988, pp. 269-276.
6. Meinheit, D. F., and Jirsa, J. O., "Shear Strength of R/C Beam-Column Connections," *Journal of Structural Engineering, ASCE*, V. 107, No. ST11, 1981, pp. 2227-2244.
7. Ehsani, M. R., and Wight, J. K., "Effect of Transverse Beams and Slab on Behavior of Reinforced Concrete Beam-to-Column Connections," *ACI JOURNAL, Proceedings V. 82, No. 2, Mar.-Apr. 1985*, pp. 188-195.
8. Tsonos, A. G.; Tegos, I. A.; and Penelis, G., "Seismic Resistance of Type 2 Exterior Beam-Column Joints Reinforced with Inclined Bars," *ACI Structural Journal*, V. 89, No. 1, Jan.-Feb. 1992, pp. 3-12.
9. Higazy, E. M.; Elnashai, A. S.; and Agbabian, M. S., "Behavior of Beam-Column Connections under Axial Column Tension," *Journal of Structural Engineering, ASCE*, V. 122, No. 5, 1996, pp. 501-511.
10. Gencoglu, M., "The Effects of Stirrups and the Extents of Regions Used SFRC in Exterior Beam-Column Joints," *Structural Engineering and Mechanics*, V. 27, No. 2, 2007, pp. 223-241.
11. Paulay, T.; Park, R.; and Priestly, M. J. N., "Reinforced Concrete Beam-Column Joints under Seismic Actions," *ACI Structural Journal*, V. 75, No. 6, Nov.-Dec. 1978, pp. 585-593.
12. Leon, R. T., "Shear Strength and Hysteretic Behavior of Beam-Column Joints," *ACI Structural Journal*, V. 87, No. 1, 1990, pp. 3-11.
13. Biddah, A., and Ghobarah, A., "Modeling of Shear Deformation and Bond Slip in Reinforced Concrete Joints," *Structural Engineering and Mechanics*, V. 7, No. 4, 1999, pp. 413-432.
14. Hegger, J.; Sherif, A.; and Roeser, W., "Nonseismic Design of Beam-Column Joints," *ACI Structural Journal*, V. 100, No. 5, Sept.-Oct. 2003, pp. 654-664.
15. Lowes, L. N., and Altoontash, A., "Modeling Reinforced-Concrete Beam-Column Joints Subjected to Cyclic Loading," *Journal of Structural Engineering, ASCE*, V. 129, No. 12, 2003, pp. 1686-1697.
16. Attaalla, S. A., "General Analytical Model for Nominal Shear Stress of Type 2 Normal and High Strength Concrete Beam-Column joints," *ACI Structural Journal*, V. 101, No. 1, Jan.-Feb. 2004, pp. 65-75.
17. Hwang, S. J.; Lee, H. J.; Liao, T. F.; Wang, K. C.; and Tsai, H. H., "Role of Hoops on Shear Strength of Reinforced Concrete Beam-Column Joints," *ACI Structural Journal*, V. 102, No. 3, May-June 2005, pp. 445-453.
18. Engindeniz, M.; Kahn, L. F.; and Zureick, A. H., "Repair and Strengthening of Reinforced Concrete Beam-Column Joints: State of the Art," *ACI Structural Journal*, V. 102, No. 2, Mar.-Apr. 2005, pp. 187-197.

19. Tsonos, A. G., "Effectiveness of CFRP-jackets in Post-Earthquake and Pre-Earthquake Retrofitting of Beam-Column Subassemblages," *Structural Engineering and Mechanics*, V. 27, No. 4, July-Aug. 2007, pp. 393-408.
20. Townsend, W. H., and Honson, R. D., "Reinforced Concrete Connection Hysteresis Loops," *Reinforced Concrete in Seismic Zones*, SP-53, N. M. Hawkins and D. Mitchell, eds., American Concrete Institute, Farmington Hills, MI, 1977, pp. 351-370.
21. Tsonos, A. G., "Improvement of the Earthquake Resistance of R/C Beam-Column Joints under the Influence of P- Δ Effect and Axial Force Variations Using Inclined Bars," *Structural Engineering and Mechanics*, V. 18, No. 4, 2004, pp. 389-410.
22. Uzumeri, S. M., "Strength and Ductility of Cast-in-Place Beam-Column Joints," *Reinforced Concrete in Seismic Zones*, SP-53, N. M. Hawkins and D. Mitchell, eds., American Concrete Institute, Farmington Hills, Michigan, 1977, pp. 293-350.
23. Pampanin, S.; Calvi, G. M.; and Moratti, M., "Seismic Behavior of R.C. Beam-Column Joints Designed for Gravity Loads." *Paper No. 726*, Proceedings of 12th European Conference on Earthquake Engineering, London, UK, 2002, 10 pp.
24. Pampanin, S.; Bolognini, D.; and Pavese, A., "Performance-Based Seismic Retrofit Strategy for Existing Reinforced Concrete Frame Systems Using Fiber-Reinforced Polymer," *Journal of Composites for Construction*, ASCE, V. 11, No. 2, 2007, pp. 211-226.
25. Abrams, D. A., "Test of Bond Between Concrete and Steel," *Bulletin No. 71*. Urbana: Engineering Experiment Station, University of Illinois at Urbana-Champaign, Urbana, IL, 1913, 238 pp.
26. Mylrea, T. D., "The Carrying Capacity of Semi-Circular Hooks," *ACI JOURNAL, Proceedings* V. 24, No. 4, Apr. 1928, pp. 240-272.
27. Stocker, M. F., and Sozen, M. A., "Investigation of Prestressed Concrete for Highway Bridges—Part V: Bond Characteristics of Prestressing Strand," *Bulletin 503*, Engineering Experiment Station, University of Illinois at Urbana-Champaign, Urbana, IL, 1970, 119 pp.
28. Fishburn, C. C., "Strength and Slip under Load of Bent-Bar Anchorage and Straight Embedment in Haydite Concrete," *ACI JOURNAL, Proceedings* V. 44, No. 4, Apr. 1947, pp. 289-308.
29. Mo, Y. L., and Chan, J., "Bond and Slip of Plain Rebars in Concrete," *Journal of Materials in Civil Engineering*, ASCE, V. 8, No. 4, 1996, pp. 208-211.
30. Kankam, L. K., "Relationship of Bond Stress, Steel Stress and Slip in Reinforcing Concrete," *Journal of Structural Engineering*, ASCE, V. 123, No. 1, 1997, pp. 79-85.
31. Cosenza, E.; Manfredi, G.; and Verderame, G. M., "Seismic Assessment of Gravity Load Designed R.C. Frames: Critical Issues in Structural Modeling," *Journal of Earthquake Engineering*, V. 6, Special Issue 1, 2002, pp. 101-122.
32. Fabbrocino, G.; Verderame, G. M.; and Manfredi, G., "Experimental Behavior of Straight and Hooked Smooth Bars in Existing R.C. Buildings," Proceedings of 12th European Conference on Earthquake Engineering, London, UK, 2002, 10 pp.
33. Feldman, L. R., and Bartlett, F. M., "Bond Strength Variability in Pullout Specimens with Plain Reinforcement," *ACI Structural Journal*, V. 102, No. 6, Nov.-Dec. 2005, pp. 860-867.
34. Bedirhanoglu, I., "The Behavior of Reinforced Concrete Columns and Joints with Low Strength Concrete under Earthquake Loads: An Investigation and Improvement," PhD thesis, Istanbul Technical University, Turkey, 2009, 700 pp.
35. Turkish Seismic Design Code, "Regulations for Buildings to be Constructed in Earthquake Prone Areas," Ankara, Turkey, 2007, 166 pp.
36. Turkish Standards Institute (TSE), "Requirements for Design and Construction of Reinforced Concrete Structures," TS500, Ankara, Turkey, 2000, 67 pp.
37. ACI Committee 318, "Building Code Requirements for Structural Concrete (ACI 318-08) and Commentary," American Concrete Institute, Farmington Hills, MI, 2008, 473 pp.

Reproduced with permission of the copyright owner. Further reproduction prohibited without permission.